Biohemistry

pubs.acs.org/biochemistry Article

Context-Sensitive Cleavage of Folded DNAs by Loop-Targeting bPNAs

Yufeng Liang, Shiqin Miao, Jie Mao, Chris DeSantis, and Dennis Bong*



Cite This: Biochemistry 2020, 59, 2410-2418



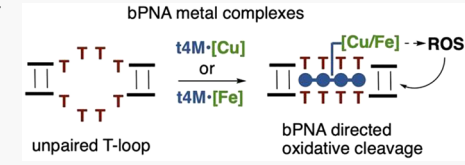
ACCESS I

Metrics & More



Supporting Information

ABSTRACT: Herein, we demonstrate context-dependent molecular recognition of DNA by synthetic bPNA iron and copper complexes, using oxidative backbone cleavage as a chemical readout for binding. Oligoethylenimine bPNAs displaying iron-EDTA or copper-phenanthroline sites were found to be efficient chemical nucleases for designed and native structured DNAs with T-rich single-stranded domains. Cleavage reactivity depends strongly on structural context, as strikingly demonstrated with DNA substrates of the form (GGGTTA)_n. This repeat sequence from the human



telomere is known to switch between parallel and antiparallel G-quadruplex (G4) topologies with a change from potassium to sodium buffer: notably, bPNA—copper complexes efficiently cleave long repeat sequences into ~22-nucleotide portions in sodium, but not potassium, buffer. We hypothesize preferential cleavage of the antiparallel topology (Na⁺) over the parallel topology (K⁺) due to the greater accessibility of the TTA loop to bPNA in the antiparallel (Na⁺) form. Similar ion-sensitive telomere shortening upon treatment with bPNA nucleases can be observed in both isolated and intracellular DNA from PC3 cells by quantitative polymerase chain reaction. Live cell treatment was accompanied by accelerated cellular senescence, as expected for significant telomere shortening. Taken together, the loop-targeting approach of bPNA chemical nucleases complements prior intercalation strategies targeting duplex and quadruplex DNA. Structurally sensitive loop targeting enables discrimination between similar target sequences, thus expanding bPNA targeting beyond simple oligo-T sequences. In addition, bPNA nucleases are cell membrane permeable and therefore may be used to target native intracellular substrates. In addition, these data indicate that bPNA scaffolds can be a platform for new synthetic binders to particular nucleic acid structural motifs.

Synthetic small molecules are known to bind specific surface features of folded macromolecules^{1,2} unlike antisense nucleic acids that target primary structure alone. However, small molecule targeting methods lack the programmability of antisense approaches, and thus, a combination of sequence and folded state targeting may yield optimal results for synthetic binders to nonduplex nucleic acids. The recognition of nonduplex structures is central to many aspects of transcription/translation regulation,³ genome maintenance,^{4,5} apoptosis, oncogenesis, and progression of neurodegenerative diseases.7 Conformationally sensitive binding creates the potential for targeting that is responsive to changes in environmental conditions or subtle mutations in primary structure. To date, selectivity rules for binding to the minor groove have been established by Dervan,8 and many other synthetic duplex intercalators and G-quadruplex 9,10 binders with limited polar interactions have been identified through design and small molecule library screens. 11-15 Despite significant progress in high-throughput searches for synthetic binders to nucleic acids, many of the molecules identified are crescent-shaped flat aromatics, ¹⁶⁻¹⁸ a consensus motif in both library hits and natural products. ^{19,20} Notably, native small molecule recognition of nucleic acids, as exemplified by aminoglycoside²¹⁻²³ antibiotics, can eschew base-stacking intercalation entirely for polar contacts and flexible shape complementarity, suggesting that considerable diversity in

small molecule/nucleic acid targeting and directed oxidation^{24,25} remains to be explored. Nonduplex regions consistently contain noncanonical or mismatched base pairs that may be uniquely targeted by molecules that can stabilize these weaker interactions.^{26–29} We have previously reported on bifacial peptide nucleic acids (bPNAs),^{30,31} a family of molecules bearing triazine^{32,33} (melamine, M) bases that triplex hybridize^{34–39} with oligo T/U sequences via the enthalpically favorable^{31,40} formation of TMT or UMU base triple stems.^{41,42} While our initial studies of bPNA focused on acidic peptide scaffolds that bind to DNA and RNA,^{43–45} we have since found that backbones composed of basic peptides,⁴⁶ peptoid,⁴⁷ polyacrylate,^{48–50} and oligoethylenimine^{51,52} can also triplex hybridize efficiently with T/U-rich nucleic acids; we apply the term "bPNA" loosely to refer to all such multimelamine scaffolds. Recently, we reported that bPNA peptides with tertiary amino branched side chains could be used to efficiently label internal RNA domains through

Received: April 30, 2020 Revised: June 8, 2020 Published: June 10, 2020





Scheme 1. General Synthetic Approach to Polyethyleneimine bPNAs, t2M and t4M^a

"Boc-ethylenediamine yields t2M-Boc via reductive alkylation with melamine acetaldehyde, which predominantly exists in hemiaminal form 1 under reaction conditions (top). Boc-tren similarly reacts with 1 to yield t4M-Boc (bottom). (a) 1, NaBH₃CN (2.2 equiv to BocNHCH₂CH₂NH₂) in methanol; (b) same as step a with 5 equiv of Boc-Tren.

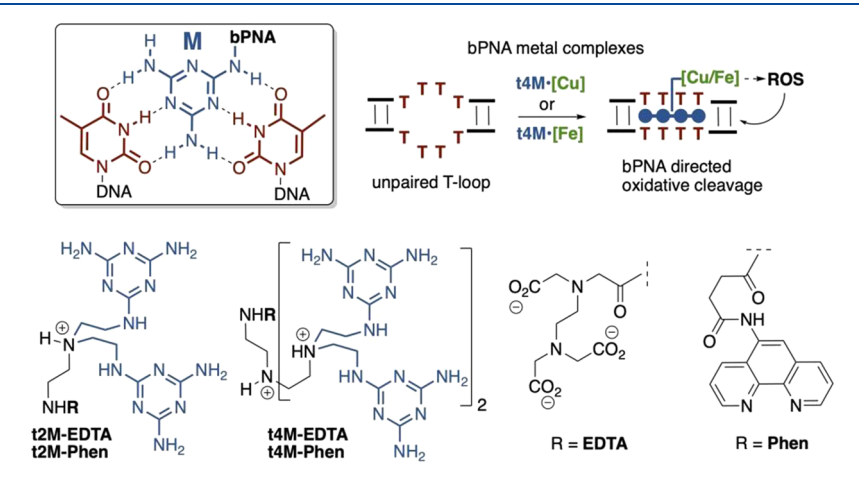


Figure 1. Melamine base triple with two thymine bases (top, inset). General scheme of bPNA copper or iron complexes binding to a single-stranded T domain, represented by a 4 × 4 internal bulge, and generating reactive oxygen species (ROS) from the metal center to cleave the DNA substrate (top right). Structures of bPNAs based on t2M and t4M scaffolds, with R groups indicating the site of linkage to EDTA and phenanthroline ligands for binding iron and copper, respectively (bottom).

replacement of 6 bp stem elements via bPNA triplex hybridization with $U_6 \times U_6$ internal bulges.⁴⁶ While this work indicated the feasibility of bPNA stem replacement as a complement to other labeling strategies,^{53–58} it also raised the possibility of bPNA selection between sequence-identical oligo-T/U internal bulges through the structural context of folded nucleic acid. Herein, we explore the notion that a simple oligoethylenimine bPNA scaffold can bind structured DNA with conformational context selectivity that extends beyond the oligo-T sequence targeted by TMT base triple formation. We designed and synthesized bPNAs bearing metal complexes capable of generating reactive oxygen species (ROS) to create a binding footprint via DNA backbone cleavage. The coupled functions of nucleic acid binding, oxidative transformation, and scission have been well-studied in the metal binding natural product family of bleomycins, 19,59 as well as synthetic systems that link targeting motifs with ROS-generating metal complexes (including bleomycins)^{60–64} and aptamers obtained via selection. 65-68 Using these established methodologies, a comparative evaluation of DNA substrates revealed that DNA reactivity is highly sensitive to both bPNA metal complex structure and the folded state of DNA, despite similar or identical base triple-targeting sites. While base stacking is no doubt important in TMT base triple formation, bPNA metal complexes uniquely target unpaired loop structures for both binding and cleavage, rather than relying exclusively on duplex intercalation and electrostatics. Indeed, the combination of sequence recognition and steric demands of the unpaired

oligo-T binding site creates a structural context that enables oligoethylenimine bPNAs to cleave short DNA sequence motifs with considerable selectivity.

■ RESULTS AND DISCUSSION

We set out to use bPNA to direct oxidative DNA cleavage⁶⁹ by Fe-EDTA and Cu-phenanthroline complexes as a sensitive readout of binding selectivity among sequences with similar thymine content. To this end, we followed the extensive literature provided by the Dervan⁶³ and Sigman⁷⁰ laboratories to install EDTA and phenanthroline sites on bPNA for generation of DNA-cleaving ROS. Tren-derived bPNA scaffolds were prepared with two (t2M) and four (t4M) melamine rings and EDTA or phenanthroline (phen) metal binding ligands (Scheme 1). Each melamine base can form a TMT base triple, 30,31 enabling targeting to 2 × 2 and 4 × 4 oligo-T internal bulges by t2M and t4M, respectively (Figure 1). Reflective of the dependence of affinity on the size of the binding interface, t4M exhibits a nanomolar range affinity for T-rich DNAs, while t2M is a micromolar binder. 51 The t2M and t4M cores are built via reductive alkylation of Bocprotected ethylenediamine starting materials⁵² with melamine acetaldehyde, 46 followed by Boc deprotection and acylation with EDTA and Phen derivatives (Scheme 1). Iron- and copper-complexed bPNAs could retain previously reported binding to T-rich DNAs in nonreducing buffers, as judged by thermal denaturation (Figures S3.1–6).

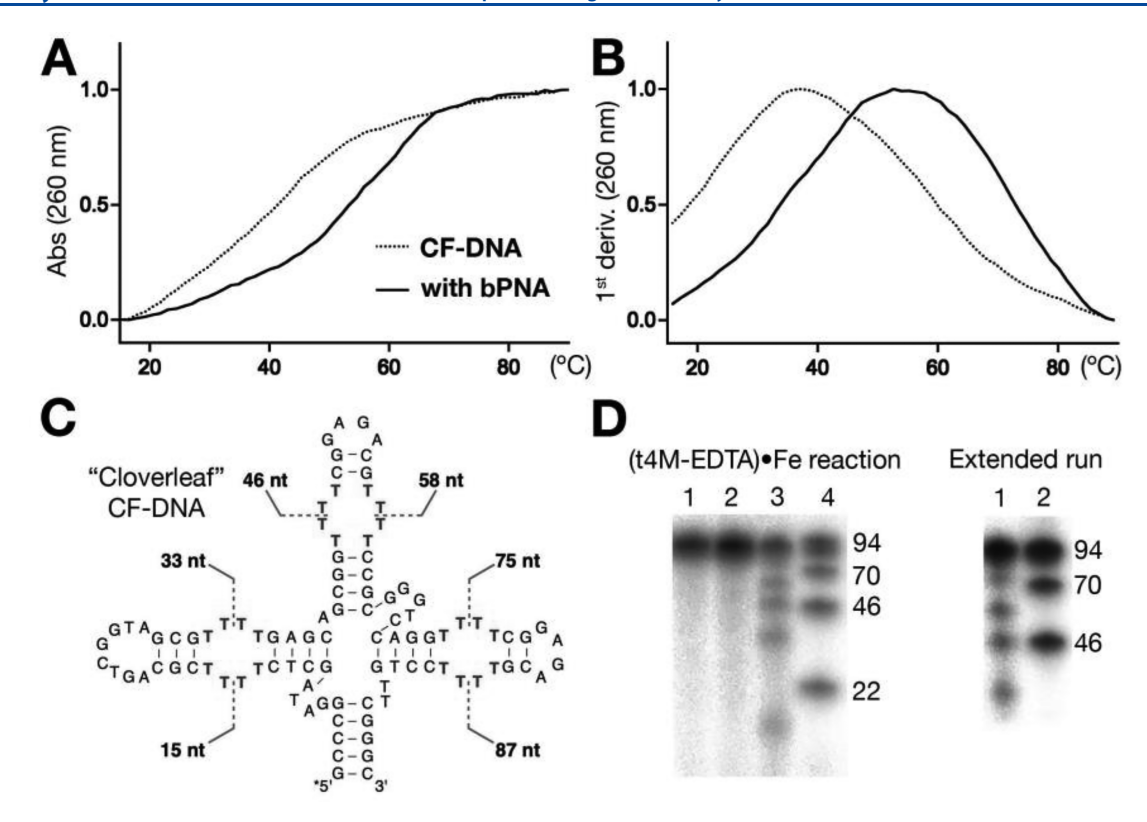


Figure 2. (A) Thermal denaturation (ultraviolet) curves of CF-DNA, (---) alone or with (t4M-EDTA)·Fe (—) as indicated, and (B) first-derivative plots of the same. Melt conditions: 2 μM DNA, 6 μM bPNA complex, 50 mM Tris-HCl (pH 7.6), and 50 mM NaCl. Samples were annealed (95 °C to room temperature) prior to melting. (C) Mfold-predicted structure of "cloverleaf" CF-DNA, with approximate cleavage sites for (t4M-EDTA)·Fe indicated, and (D) denaturing DNA gel analysis: lane 1, CF-DNA, no treatment; lane 2, with EDTA·Fe; lane 3, with (t4M-EDTA)·Fe; lane 4, ladder of 22-, 46-, 70-, and 94-nucleotide CF-DNA fragments. Right gel: lane 1, extended run of (t4M-EDTA)·Fe cleavage reaction shown for the sake of clarity; lane 2, ladder. Reaction conditions: 50 mM Tris-HCl (pH 7.6), 50 mM NaCl, 4 mM DTT, 500 nM 5′-radiolabeled (³²P) DNA, and iron complex. The reaction was quenched and analyzed after 6 h.

Site-directed DNA cleavage was initially tested by reacting (t4M-EDTA)·Fe with an Mfold⁷¹-designed four-armed "cloverleaf" DNA structure (CF-DNA), wherein three arms contain 4 × 4 oligo-T internal bulges buttressed by duplex stems (Figure 2C). Treatment with (t4M-EDTA)·Fe under ROS-generating conditions rapidly fragmented full-length CF-DNA into a discrete set of smaller strands corresponding to cleavage on both sides of each of the three internal bulge sites, verified using a ladder of DNA sequences of known length. This cleavage pattern is consistent with production of ROS at the t4M binding site (Figure 2D). Sequences with identical oligo-T domains but without a supporting duplex structure were not detectably cleaved by (t4M-EDTA) Fe under the same conditions, suggesting that a prestructured oligo-T is required for oxidative scission, most likely through increased binding efficiency (Figure S4.2.3,4). Although oligoamines have been reported to cleave RNA through metal-ion independent mechanisms, 72,73 the bPNA skeleton itself did not cause DNA strand breaks. Supportive of the notion that a 4 × 4 internal T bulge can generally be cleaved on both strands by (t4M-EDTA)·Fe, an analogous CF-DNA scaffold bearing a single internal bulge 4 × 4 oligo-T site yielded two products upon oxidation that correspond to cleavage on either side of the internal bulge (Figure S10). Neither (t2M-EDTA)·Fe nor (t2M-Phen)₂·Cu yielded significant cleavage under the same conditions with either 2×2 or 4×4 oligo-T internal bulge; this is in part attributable to insufficient t2M-DNA binding affinity. However, despite the higher binding affinity, we

observed that (t4M-Phen)₂·Cu also did not detectably cleave CF-DNA, suggesting an inherent reactivity difference between the iron— and copper—bPNA complexes. The metal complexes have distinct DNA oxidation mechanisms. Fe·EDTA produces diffusible ROS, while Cu-Phen reacts with DNA as a copperoxo species⁷⁴ that remains bound to the bPNA scaffold. The close approach of the copper center to the DNA backbone likely results in higher cleavage selectivity for conformations that minimize steric demand. Ligand dimerization to form (t4M-Phen)₂·Cu would further increase steric barriers to cleavage and require that the cleavage site be between the two bPNA binding sites, even as it increases the DNA affinity. To probe our hypothesis, we designed a DNA duplex substrate with two coaxial 4×4 T internal bulges separated by a 6 bp stem (coaxial internal bulge or CIB-DNA) (Figure 3A). This design presumed simultaneous binding of t4M motifs to the two 4 × 4 T bulges and would be expected to direct DNA cleavage between the two binding sites at the approximate footprint of the copper center. Gratifyingly, this designed substrate was cleaved by both (t4M-EDTA)·Fe and (t4M-Phen)₂·Cu, but with notably distinct cleavage patterns (Figure 3B). While the EDTA complex yielded DNA fragments corresponding to cleavage at both internal bulges, the (t4M-Phen)2·Cu complex produced a single cleavage fragment of intermediate length, consistent with cleavage between the two sites. Interestingly, we also found that CIB-DNA cleavage by the copper complex requires an unpaired site between the two internal bulges; replacement of the tandem CC mismatch site

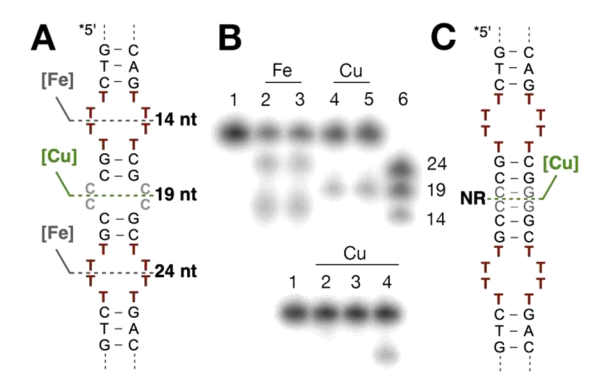


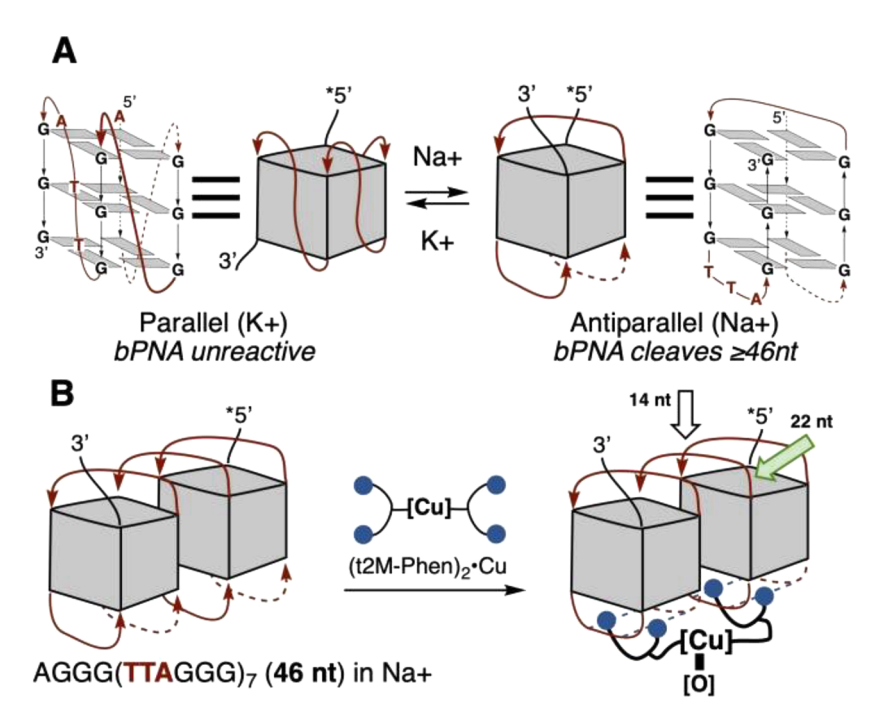
Figure 3. (A) Mfold-predicted structure of coaxial internal bulge (CIB) DNA with approximate cleavage sites indicated for (t4M-EDTA)·Fe and (t4M-Phen)₂·Cu and (B) denaturing gel analysis: lane 1, CIB-DNA, no treatment; lane 2, with (t4M-EDTA)·Fe in 50 mM NaCl; lane 3, with (t4M-EDTA)·Fe in 50 mM KCl; lane 4, with (t4M-Phen)₂·Cu in 50 mM NaCl; lane 5, (t4M-Phen)₂·Cu in 50 mM KCl; lane 6, DNA ladder of CIB-DNA fragments. Bottom gel: lane 1, CIB-DNA with a C4 internal bulge replaced with a 2 bp stem (CIB-bp); lane 2, labeled CIB-bp single strand with (t4M-Phen)₂·Cu as in top gel; lane 3, same as lane 2 but with a CIB-bp duplex; lane 4, with (t4M-Phen)₂·Cu in 50 mM NaCl. (C) Mfold-predicted structure of CIB-bp DNA with no reaction (NR) indicated at the cleavage site. Reaction conditions: 50 mM Tris-HCl (pH 7.6), 2 mM DTT, 500 nM 5'-radiolabeled (³²P) DNA and metal complex, and indicated NaCl or KCl. The reaction was quenched and analyzed after 6 h.

in CIB-DNA with CG base pairs completely blocked DNA cleavage (Figure 3). Thus, substrate reactivity may be further tuned by installing a mispaired site (eg-CC) between the two bPNA binding sites, thereby directing cleavage to a specific location. Overall, these cleavage profiles reflect a sensitivity to

bPNA binding mode and DNA folded state that extends target selectivity beyond the oligo-T internal bulge sequence and, importantly, provide a blueprint for the design of chemical nuclease digestion sites.

The successful design of bPNA-reactive folded DNAs prompted examination of native T-rich folded DNAs, such as the human telomere repeat sequence, as substrates for bPNAdirected scission. Telomeric DNA and other native nucleic acids have been targeted for binding⁷⁵ and oxidative cleavage in many prior studies, including those using synthetic and natural products 10,69,76-78 as well as metalated aminoglycosides.⁷⁹ The AGGG(TTAGGG)₃ sequence has been found to switch between parallel⁸⁰ and antiparallel⁸¹ G4 folds upon exchanging potassium for sodium buffer; this change in topology significantly impacts how the TTA loops are presented. In the parallel (K+) form, the TTA loops are on the side of the G4 stack, and in the antiparallel (Na⁺) form, the loops are on the top and bottom of the G4 stack in a "basket handle" conformation (Scheme 2). Telomere sequence DNAs of increasing length were studied, from the minimal 22nucleotide folding unit of AGGG(TTAGGG)3, which forms three stacked G4 layers, to AGGG(TTAGGG)₇, AGGG-(TTAGGG)₁₁, and AGGG(TTAGGG)₁₅. We found that $(t2M-Phen)_2\cdot Cu$ increased the melting temperature (T_m) of the folded 94-nucleotide telomere sequence (Figure 4) while no change in $T_{\rm m}$ was observed with the methylated analogue, (t2MMe-Phen)2·Cu. Interestingly, while t2M-Phen increased the $T_{\rm m}$ (+2 °C), the largest increase in $T_{\rm m}$ was observed with both copper and ligand (+7 °C), while copper itself did not elicit a change (Figure 4 and Figure S3.4); this is consistent with ligand dimerization at the copper center increasing affinity through multivalency.

Scheme 2. (A) Parallel and Antiparallel G4 Folds of the Same Telomere Sequence $AGGG(TTAGGG)_n$ That Form in Potassium and Sodium Buffers, Respectively, Established for n=3 and (B) Schematic Illustration of How Longer Repeat Sequences (n=7, 11, or 15) Could Form Folded Structures That Present the TTA Loops on One Face of the Structure, Enabling Binding of (t2M-Phen)₂·Cu and Cleavage at the Proximal Loops, Yielding ~22-Nucleotide (green arrow) and ~14-Nucleotide (white arrow) Products as the Major and Minor Products, Respectively



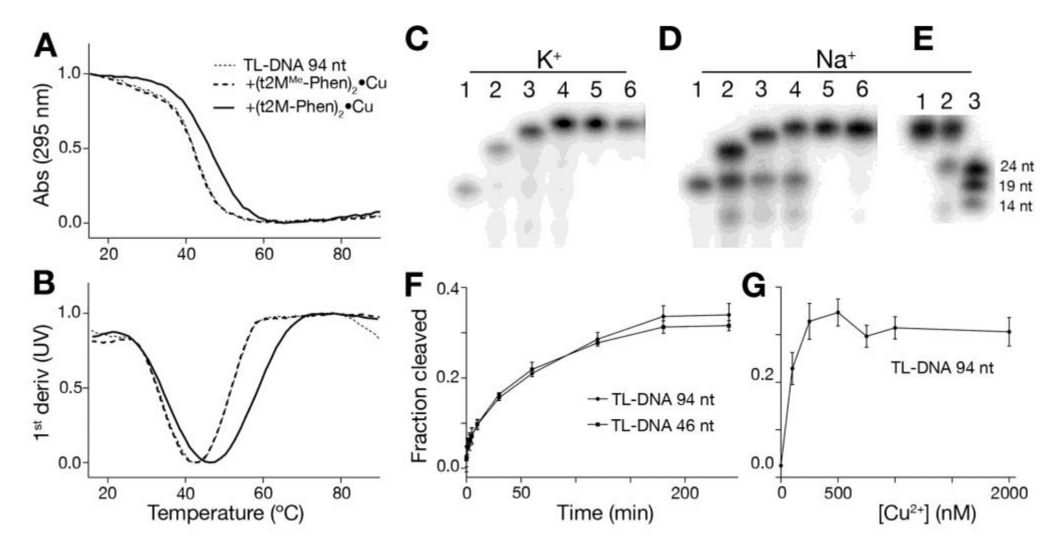


Figure 4. (A) Thermal denaturation (ultraviolet) curves of TL-DNA (94 nucleotides) alone or with bPNA copper complexes as indicated and (B) first-derivative plots of the same. Melt conditions: $2 \mu M$ DNA, $3.75 \mu M$ copper complex, 50 mM Tris-HCl (pH 7.6), and 30 mM NaCl. Samples were annealed (95 °C to room temperature) prior to melting. The bPNA $t2M^{\text{Me}}$ -Phen has permethylated melamine. (C) Denaturing gel analysis of cleavage reactions of telomere repeat (TL-DNA) sequences $AGGG(TTAGGG)_n$ with $(t2M\text{-Phen})_2$ ·Cu in 30 mM KCl buffer: lane 1, n = 3, 22 nucleotides; lane 2, n = 7, 46 nucleotides; lane 3, n = 11, 70 nucleotides; lane 4, n = 15, 94 nucleotides; lane 5, 94 nucleotides with (t2M-EDTA)·Fe; lane 6, 94 nucleotides with (t4M-EDTA)·Fe. (D) Same as panel C with 30 mM NaCl instead of KCl. (E) Gel analysis of TL-DNA (46 nucleotides) in 30 mM NaCl buffer: lane 1, untreated 46 nucleotides; lane 2, after treatment with (t2M-Phen)₂·Cu; lane 3, DNA ladder of TL-DNA fragments. (F) Time-dependent cleavage of the indicated TL-DNAs from gel quantitation. (G) Cleavage of 94-nucleotide TL-DNA as a function of copper sulfate concentration with 1 μ M t2M-Phen. DNAs were 32 P-labeled (5'). General reaction conditions: 500 nM DNA, 1 equiv of bPNA complex, 50 mM Tris-HCl (pH 7.6), and 4 mM DTT, 6 h. Reactions were run in triplicate for each time point and copper concentration.

Remarkably, both copper—bPNA complexes (t4M-Phen)₂·Cu and (t2M-Phen)₂·Cu could cleave these telomere repeat sequences (with the exception of the 22-nucleotide DNA), but only in sodium and not in potassium buffer. Neither (t4M-EDTA)·Fe nor (t2M-EDTA)·Fe elicited detectable DNA fragmentation. Furthermore, although the t2M-targeting motif showed poor cleavage activity with other substrates, (t2M-Phen)₂·Cu was the most efficient cleavage reagent (35%) against the telomere sequences, with activity exceeding that of (t4M-Phen)₂·Cu (25%), but exclusively in sodium buffer, with undetectable reaction in potassium buffer (Table 1).

Table 1. bPNA-DNA Reactivities and Cleavage Yields^a

bPNA	CF	CIB	TL/K^{+}	TL/Na+
(t2M-EDTA)·Fe	NR	NR	NR	NR
(t4M-EDTA)·Fe	78%	40%	NR	NR
$(t2M-Phen)_2\cdot Cu$	NR	NR	NR	35%
$(t4M-Phen)_2\cdot Cu$	NR	13%	NR	25%

"All reactions were performed for 6 h in 50 mM Tris-HCl (pH 7.6) with 500 nM CF, CIB, or TL-DNA and 1 equiv of a metal complex. NR = no reaction. Telomere (TL) DNA reactions were performed in either 30 mM NaCl or 30 mM KCl, while all other reactions were performed in 50 mM NaCl. Reactions were started by addition of DTT to a final concentration of 4 or 2 mM for the reaction of CIB-DNA with(t4M-Phen)₂·Cu.

Interestingly, (t2M-Phen)₂·Cu fragmented the 46-, 70-, and 94-nucleotide DNAs into a common major product approximately 22 nucleotides in length, which is the minimal G4 folding unit. The 46- and 94-nucleotide DNAs are cleaved at similar rates (Figure 4F), suggesting that the DNA is saturated by bPNA under these conditions. Furthermore, though all reactions were analyzed after 6 h, both reactions reach the maximum cleavage yield in 2 h, most likely due to depletion of

dithiothreitol (DTT) by this time. The reaction yield and rate were found to increase from 0 to 30 mM NaCl; above this salt concentration, reactivity decreased, most likely due to electrostatic screening of bPNA binding (Figure S14). In all cases, reaction with TL-DNA was observed only in sodiumcontaining buffer. In contrast, CIB-DNA was cleaved by (t4M-Phen)2·Cu in both sodium and potassium buffer, indicating that K⁺ does not inherently inhibit reactivity (Figure 3B). While (t2M-Phen)₂·Cu exhibited no DNA cleavage activity against the CIB-DNA substrate, we attribute this to weak binding. These data support the notion that the antiparallel Gquadruplex fold favored in sodium buffer is more susceptible to oxidative backbone cleavage by bPNA-copper complexes than the parallel G-quadruplex formed in potassium buffer. We hypothesize that the origin of this selectivity derives from the greater steric accessibility of both the TTA loop and the DNA backbone itself in the antiparallel G-quadruplex fold relative to the parallel form. Presentation of multiple TTA loops on one face of the antiparallel (Na⁺) G4 structure may enable binding of the (t2M-Phen)₂·Cu dimer in a way that is geometrically favorable for the copper-bound oxo species to attack the DNA backbone between two minimal folding (22-nucleotide) units; presumably, this approach of the metal center to DNA is not facile in the parallel (K^{+}) G4 (Scheme 2). Importantly, sequences that fold into G-quadruplexes, 82,83 (GGGT)₄ and (GGGT)₈, but lack the TTA loop did not react with bPNA copper complexes, indicating that cleavage is directed by loop recognition rather than G4 stacking. Binding of bPNA to DNA thermally stabilizes the G4 fold in both Na⁺ and K⁺ (Supporting Information), but (t2M-Phen), Cu binding leads to cleavage in only Na⁺ buffer (Figure 4). Our prior cleavage study of CIB-DNA (Figure 3) indicated that the copperphenanthroline bPNA is capable of cleaving DNA in both sodium and potassium buffers, suggesting that the DNA folded state is driving selectivity. Furthermore, even though the 22-

nucleotide DNA was unreactive, the 48-, 70-, and 94nucleotide DNAs produced minor products shorter than the ~22-nucleotide major common product. Comparison with a DNA ladder indicated a smaller fragment of \sim 13 nucleotides; in our model of DNA cleavage, this would indicate cleavage at two TTA loops that are 8 nucleotides apart but spatially close to one another in the antiparallel G4 fold, with preferential cleavage at the second TTA loop (Scheme 2). Remarkably, even though (t4M-EDTA)·Fe readily cleaves 4 × 4 internal bulges in the cloverleaf and coaxial internal bulge designs (Table 1), it does not detectably cleave telomere sequence DNA, nor does it elicit a shift in thermal stability (Figure S6). Together with optimal observed telomere sequence cleavage at a 2:1 ligand:copper ratio (Figure 4G), this suggests that ligand dimerization at the metal center assists in binding. In addition, the greater activity of (t2M-Phen)2·Cu supports the notion that only two of the four melamine bases on (t4M-Phen)₂·Cu are needed in binding to each set of two TTA loops, with the remaining melamine bases creating steric hindrance. Consistent with this, the 22-nucleotide sequence, which has only three of the four TTA loops needed to bind (t2M-Phen)2.Cu, does not exhibit an increase in $T_{\rm m}$ on treatment with bPNAs.

Cleavage data for this range of synthetic substrates (Table 1) indicate a considerable range of reactivity for similar T-rich sequences as a function of minor modifications in bPNA structure and metal complex; these effects are amplified for the telomere repeat sequence, wherein only one conformation of the same sequence is reactive with bPNA.

The (t2M-Phen), Cu complex also cleaved genomic DNA isolated from PC3 cells with similar preferential reactivity in Na⁺ buffer over K⁺ buffer, decreasing the telomere length by ~40% in 6 h (Figure 5A). This confirmed bPNA nuclease activity with native telomeric sequences in heterogeneous samples and prompted investigation of intracellular activity. We were encouraged to find that the oligoethyleneimine bPNA copper complex was taken up by PC3 cells without carriers, as judged by intracellular copper transport (Figure 5B). Treatment of PC3 cells with (t2M-Phen)₂·Cu followed by washing and copper quantification by ICP-MS revealed significant bPNA-dependent copper uptake. The scope and determinants of bPNA transport are currently under investigation. With these data supporting cell penetration, we tested the extent to which copper-bound bPNA nuclease could shorten telomeres in PC3 cells in culture. Cells were treated with (t2M-Phen)₂. Cu and then harvested at different time points, and DNA was isolated and telomere length analyzed by quantitative polymerass chain reaction (qPCR).^{84–86} Gratifyingly, we found a significant (>50%) decrease in telomere length (Figure 5C) under conditions where the bPNA-copper complex has minimal cellular toxicity (Figure S21). Telomere shortening was further validated by a lysozyme (X-gal) assay for cellular senescence, 87 which reported a 70% increase in the number of senescent cells following treatment with (t2M-Phen)₂·Cu (Figure 5D). Though Phen-Cu itself exhibits known toxicity and a 25% increase in senescence, the combination with bPNA targeting results in a substantial above-background effect. Additionally, though the cellular environment is not exclusively sodium or potassium, we hypothesize that a dynamic intracellular telomere folded state⁸⁸ allows bPNA to capture the antiparallel G-quadruplex conformation. Overall, it appears that the (t2M-Phen)₂·Cu complex takes advantage of a combination of TTA loop binding and stacking with the G4 surface to bind the folded telomere at two sites, cleaving

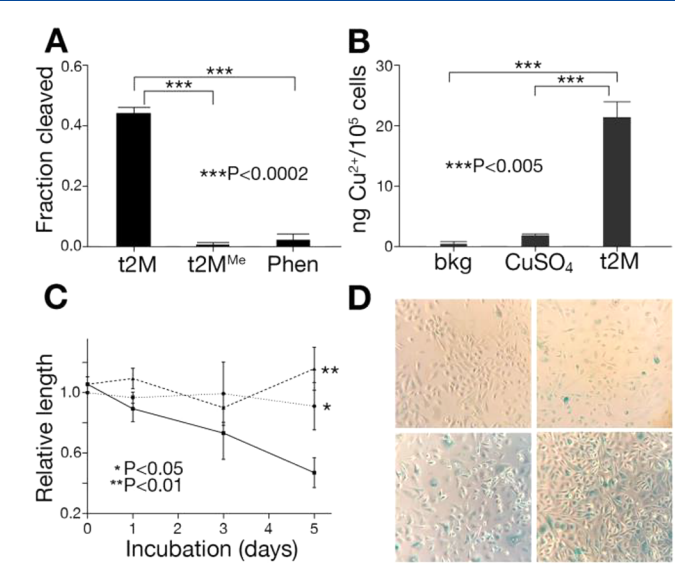


Figure 5. (A) qPCR analysis of telomere domain cleavage of genomic DNA isolated from PC3 cells under NaCl buffer conditions [50 mM Tris-HCl (pH 7.6), 4 mM DTT, and 30 mM NaCl] with the indicated bPNA-Phen or phenanthroline Cu complexes. (B) ICP-MS analysis of intracellular copper following treatment with the t2M-Phen complex as indicated. (C) Decrease in telomere length in PC3 cells following treatment of live cells for the indicated reagents and incubation times. (D) Cellular senescence of PC3 cells estimated using the X-gal assay for lysozyme activity (blue): (top left) untreated, 1%; (top right) with Phen₂·Cu, 30%; (bottom left) with (t2M^{Me}-Phen)₂·Cu, 40%; (bottom right) (t2M-Phen)₂·Cu, 70%. All experiments performed in triplicate with P values as indicated, with the exception of the senescence assay, which was performed in duplicate.

between them in a manner similar to that of CIB-DNA. This targeting method is unique among reagents that target the G-quadruplex fold of the telomere repeat; previously reported synthetic binders typically rely on electrostatics and G4 stacking without TTA loop binding elements. Notably, the $(t2M-Phen)_2$ ·Cu mode of action appears to be more efficient at cleaving the antiparallel telomere than (t2M-EDTA)·Fe or (t4M-EDTA)·Fe, suggesting that Phen/G4 stacking and bidentate binding could be assisting in backbone scission.

CONCLUSIONS

Taken together, this study demonstrates that the folded state of nucleic acids can amplify binding selectivity for small synthetic molecules, as reported by oxidative DNA backbone cleavage. While the primary mode of bPNA-DNA recognition is formation of TMT base triples, these data indicate that bPNA nuclease binding and activity depend strongly on the folded state context in which the oligo-T sequence is presented. This is vividly illustrated by the selective reaction of bPNA nucleases with the antiparallel G4 conformation of the telomere repeat sequence but not the parallel G4. Indeed, reactivity may be toggled on in Na⁺ (antiparallel G4) and off in K⁺ (parallel G4). In engineered DNAs, the placement of the T loop/bulge binding site, the number of binding sites, and the bPNA nuclease structure itself can direct different reaction outcomes, all with the same primary sequence binding site. Therefore, although the melamine base itself is limited to targeting oligo-T sites, bPNA and DNA structural features significantly augment binding selectivity, in much the same way that molecular interactions between small molecules and protein motifs are context-dependent. Additionally, these

bPNA nuclease systems exploit mechanistic differences in ROS generation⁷⁴ by Fe·EDTA and Cu·Phen complexes to further increase selectivity. We hypothesize that the need for bPNA to bind to conformationally labile 89 unpaired loop/bulge oligo-T domains renders bPNA targeting particularly sensitive to the demands of local secondary structure that could collapse the oligo-T site into an inaccessible conformation. This steric sensitivity is compounded in the Cu-Phen system, which appears to require at minimum two bPNA binding sites and an unpaired site between the two sites for cleavage. Overall, metal complex-modified bPNAs functionally expand the catalog of chemical nucleases^{24,62} with context-sensitive reaction, tunable cleavage site selectivity, and applicability to intracellular targets such as the human telomere sequence. We believe the results presented herein establish the potential for new contextselective bPNA interactions with DNA and RNA folded structures that extend beyond primary sequence recognition and specificity. These results suggest that bPNA scaffolds could serve as a platform for new synthetic binders to particular nucleic acid structural motifs, thus providing a design-based counterpoint to library-based screening approaches.

ASSOCIATED CONTENT

5 Supporting Information

The Supporting Information is available free of charge at https://pubs.acs.org/doi/10.1021/acs.biochem.0c00362.

General procedures, sequences, additional thermal denaturation data, oxidative cleavage raw and processed data, cellular toxicity data, and compound characterization (PDF)

AUTHOR INFORMATION

Corresponding Author

Dennis Bong — Department of Chemistry & Biochemistry and Center for RNA Biology, The Ohio State University, Columbus, Ohio 43210, United States; ⊚ orcid.org/0000-0003-3778-9183; Email: bong.6@osu.edu

Authors

Yufeng Liang — Department of Chemistry & Biochemistry and Center for RNA Biology, The Ohio State University, Columbus, Ohio 43210, United States

Shiqin Miao — Department of Chemistry & Biochemistry and Center for RNA Biology, The Ohio State University, Columbus, Ohio 43210, United States

Jie Mao – Department of Chemistry & Biochemistry and Center for RNA Biology, The Ohio State University, Columbus, Ohio 43210, United States

Chris DeSantis – Department of Chemistry & Biochemistry and Center for RNA Biology, The Ohio State University, Columbus, Ohio 43210, United States

Complete contact information is available at: https://pubs.acs.org/10.1021/acs.biochem.0c00362

Funding

This work was supported in part by funding from the National Institutes of Health (GM111995-01A1 to D.B.), the National Aeronautics and Space Administration (GRT00044810 to D.B.), and the National Science Foundation (DMR 1802432 to D.B.). S.M. acknowledges fellowship support from the Center of RNA Biology of The Ohio State University.

Notes

The authors declare no competing financial interest.

REFERENCES

- (1) Wang, F., and Fesik, S. W. (2015) Discovery of Inhibitors of Protein--Protein Interactions Using Fragment-Based Methods. *Fragment-based Drug Discovery: Lessons and Outlook*, Wiley.
- (2) Arkin, M. R., and Wells, J. A. (2004) Small-molecule inhibitors of protein-protein interactions: progressing towards the dream. *Nat. Rev. Drug Discovery* 3, 301–317.
- (3) Jing, Q., Huang, S., Guth, S., Zarubin, T., Motoyama, A., Chen, J., Di Padova, F., Lin, S.-C., Gram, H., and Han, J. (2005) Involvement of microRNA in AU-rich element-mediated mRNA instability. *Cell* 120, 623–634.
- (4) Nandakumar, J., and Cech, T. R. (2013) Finding the end: recruitment of telomerase to telomeres. *Nat. Rev. Mol. Cell Biol.* 14, 69–82.
- (5) Qiao, F., and Cech, T. R. (2008) Triple-helix structure in telomerase RNA contributes to catalysis. *Nat. Struct. Mol. Biol.* 15, 634–640.
- (6) Ambros, V. (2004) The functions of animal microRNAs. *Nature* 431, 350–355.
- (7) King, O. D., Gitler, A. D., and Shorter, J. (2012) The tip of the iceberg: RNA-binding proteins with prion-like domains in neuro-degenerative disease. *Brain Res.* 1462, 61–80.
- (8) Urbach, A. R., and Dervan, P. B. (2001) Toward rules for 1:1 polyamide: DNA recognition. *Proc. Natl. Acad. Sci. U. S. A.* 98, 4343–4348.
- (9) Balasubramanian, S., Hurley, L. H., and Neidle, S. (2011) Targeting G-quadruplexes in gene promoters: a novel anticancer strategy? *Nat. Rev. Drug Discovery 10*, 261–275.
- (10) Neidle, S. (2017) Quadruplex nucleic acids as targets for anticancer therapeutics. *Nat. Rev. Chem.* 1, 0041.
- (11) Rzuczek, S. G., Colgan, L. A., Nakai, Y., Cameron, M. D., Furling, D., Yasuda, R., and Disney, M. D. (2017) Precise small-molecule recognition of a toxic CUG RNA repeat expansion. *Nat. Chem. Biol.* 13, 188–193.
- (12) Velagapudi, S. P., Cameron, M. D., Haga, C. L., Rosenberg, L. H., Lafitte, M., Duckett, D. R., Phinney, D. G., and Disney, M. D. (2016) Design of a small molecule against an oncogenic noncoding RNA. *Proc. Natl. Acad. Sci. U. S. A. 113*, 5898–5903.
- (13) Barros, S. A., and Chenoweth, D. M. (2014) Recognition of nucleic acid junctions using triptycene-based molecules. *Angew. Chem., Int. Ed.* 53, 13746–13750.
- (14) Donlic, A., Morgan, B. S., Xu, J. L., Liu, A., Roble, C., Jr, and Hargrove, A. E. (2018) Discovery of Small Molecule Ligands for MALAT1 by Tuning an RNA-Binding Scaffold. *Angew. Chem., Int. Ed.* 57, 13242–13247.
- (15) Felsenstein, K. M., Saunders, L. B., Simmons, J. K., Leon, E., Calabrese, D. R., Zhang, S., Michalowski, A., Gareiss, P., Mock, B. A., and Schneekloth, J. S., Jr. (2016) Small Molecule Microarrays Enable the Identification of a Selective, Quadruplex-Binding Inhibitor of MYC Expression. *ACS Chem. Biol.* 11, 139–148.
- (16) Abulwerdi, F. A., Xu, W., Ageeli, A. A., Yonkunas, M. J., Arun, G., Nam, H., Schneekloth, J. S., Dayie, T. K., Spector, D., Baird, N., and Le Grice, S. F. J. (2019) Selective small molecule targeting of a triple helix encoded by the long non-coding RNA, MALAT1. ACS Chem. Biol. 14, 223.
- (17) Haniff, H. S., Graves, A., and Disney, M. D. (2018) Selective Small Molecule Recognition of RNA Base Pairs. *ACS Comb. Sci.* 20, 482–491.
- (18) Disney, M. D. (2019) Targeting RNA with Small Molecules To Capture Opportunities at the Intersection of Chemistry, Biology, and Medicine. *J. Am. Chem. Soc.* 141, 6776–6790.
- (19) Stubbe, J., and Kozarich, J. W. (1987) Mechanisms of bleomycin-induced DNA degradation. *Chem. Rev.* 87, 1107–1136.
- (20) Chen, X., Ramakrishnan, B., Rao, S. T., and Sundaralingam, M. (1994) Binding of two distamycin A molecules in the minor groove of an alternating B-DNA duplex. *Nat. Struct. Biol.* 1, 169–175.

- (21) Magnet, S., and Blanchard, J. S. (2005) Molecular insights into aminoglycoside action and resistance. *Chem. Rev.* 105, 477–498.
- (22) Griffey, R. H., Hofstadler, S. A., Sannes-Lowery, K. A., Ecker, D. J., and Crooke, S. T. (1999) Determinants of aminoglycoside-binding specificity for rRNA by using mass spectrometry. *Proc. Natl. Acad. Sci. U. S. A.* 96, 10129–10133.
- (23) Tor, Y., Hermann, T., and Westhof, E. (1998) Deciphering RNA recognition: aminoglycoside binding to the hammerhead ribozyme. *Chem. Biol.* 5, R277–83.
- (24) Cowan, J. A. (2001) Chemical nucleases. Curr. Opin. Chem. Biol. 5, 634-642.
- (25) Sreedhara, A., Freed, J. D., and Cowan, J. A. (2000) Efficient Inorganic Deoxyribonucleases. Greater than 50-Million-Fold Rate Enhancement in Enzyme-Like DNA Cleavage. *J. Am. Chem. Soc.* 122, 8814—8824.
- (26) SantaLucia, J., Jr., and Hicks, D. (2004) The thermodynamics of DNA structural motifs. *Annu. Rev. Biophys. Biomol. Struct.* 33, 415–440
- (27) SantaLucia, J., Jr., and Turner, D. H. (1997) Measuring the thermodynamics of RNA secondary structure formation. *Biopolymers* 44, 309–319.
- (28) Xia, T., SantaLucia, J., Burkard, M. E., Kierzek, R., Schroeder, S. J., Jiao, X., Cox, C., and Turner, D. H. (1998) Thermodynamic Parameters for an Expanded Nearest-Neighbor Model for Formation of RNA Duplexes with Watson-Crick Base Pairs. *Biochemistry* 37, 14719—14735
- (29) Mathews, D. H., Sabina, J., Zuker, M., and Turner, D. H. (1999) Expanded sequence dependence of thermodynamic parameters improves prediction of RNA secondary structure. *J. Mol. Biol.* 288, 911–940.
- (30) Zeng, Y., Pratumyot, Y., Piao, X., and Bong, D. (2012) Discrete assembly of synthetic peptide-DNA triplex structures from polyvalent melamine-thymine bifacial recognition. *J. Am. Chem. Soc. 134*, 832–835
- (31) Piao, X., Xia, X., and Bong, D. (2013) Bifacial Peptide Nucleic Acid Directs Cooperative Folding and Assembly of Binary, Ternary, and Quaternary DNA Complexes. *Biochemistry* 52, 6313–6323.
- (32) Mittapalli, G. K., Reddy, K. R., Xiong, H., Munoz, O., Han, B., De Riccardis, F., Krishnamurthy, R., and Eschenmoser, A. (2007) Mapping the landscape of potentially primordial informational oligomers: oligodipeptides and oligodipeptiods tagged with triazines as recognition elements. *Angew. Chem., Int. Ed.* 46, 2470–2477.
- (33) Sanjayan, G. J., Pedireddi, V. R., and Ganesh, K. N. (2000) Cyanuryl-PNA monomer: synthesis and crystal structure. *Org. Lett.* 2, 2825.
- (34) Thadke, S. A., Perera, J. D. R., Hridya, V. M., Bhatt, K., Shaikh, A. Y., Hsieh, W.-C., Chen, M., Gayathri, C., Gil, R. R., Rule, G. S., Mukherjee, A., Thornton, C. A., and Ly, D. H. (2018) Design of Bivalent Nucleic Acid Ligands for Recognition of RNA-Repeated Expansion Associated with Huntington's Disease. *Biochemistry* 57, 2094–2108.
- (35) Chen, H., Meena, and McLaughlin, L. W. (2008) A Januswedge DNA triplex with A-W1-T and G-W2-C base triplets. *J. Am. Chem. Soc.* 130, 13190–13191.
- (36) Largy, E., Liu, W., Hasan, A., and Perrin, D. M. (2013) Base-Pairing Behavior of a Carbocyclic Janus-AT Nucleoside Analogue Capable of Recognizing A and T within a DNA Duplex. *ChemBioChem* 14, 2199–2208.
- (37) Shin, D., and Tor, Y. (2011) Bifacial Nucleoside as a Surrogate for Both T and A in Duplex DNA. J. Am. Chem. Soc. 133, 6926–6929.
- (38) Branda, N., Kurz, G., and Lehn, J.-M. (1996) JANUS WEDGES: a new approach towards nucleobase-pair recognition. *Chem. Commun.*, 2443–2444.
- (39) Zengeya, T., Gupta, P., and Rozners, E. (2012) Triple-helical recognition of RNA using 2-aminopyridine-modified PNA at physiologically relevant conditions. *Angew. Chem., Int. Ed.* 51, 12593–12596.
- (40) Ma, M., and Bong, D. (2011) Determinants of cyanuric acid and melamine assembly in water. *Langmuir* 27, 8841–8853.

- (41) Arambula, J. F., Ramisetty, S. R., Baranger, A. M., and Zimmerman, S. C. (2009) A simple ligand that selectively targets CUG trinucleotide repeats and inhibits MBNL protein binding. *Proc. Natl. Acad. Sci. U. S. A. 106*, 16068–16073.
- (42) Lange, R. F. M., Beijer, F. H., Sijbesma, R. P., Hooft, R. W. W., Kooijman, H., Spek, A. L., Kroon, J., and Meijer, E. W. (1997) Crystal Engineering of Melamine-Imide Complexes; Tuning the Stoichiometry by Steric Hindrance of the Imide Carbonyl Groups. *Angew. Chem., Int. Ed. Engl.* 36, 969–971.
- (43) Piao, X., Xia, X., Mao, J., and Bong, D. (2015) Peptide ligation and RNA cleavage via an abiotic template interface. *J. Am. Chem. Soc.* 137, 3751–3754.
- (44) Xia, X., Piao, X., and Bong, D. (2014) Bifacial peptide nucleic acid as an allosteric switch for aptamer and ribozyme function. *J. Am. Chem. Soc.* 136, 7265–7268.
- (45) Xia, X., Piao, X., Fredrick, K., and Bong, D. (2014) Bifacial PNA complexation inhibits enzymatic access to DNA and RNA. *ChemBioChem* 15, 31–36.
- (46) Miao, S., Liang, Y., Marathe, I., Mao, J., DeSantis, C., and Bong, D. (2019) Duplex Stem Replacement with bPNA+ Triplex Hybrid Stems Enables Reporting on Tertiary Interactions of Internal RNA Domains. J. Am. Chem. Soc. 141, 9365–9372.
- (47) Mao, J., and Bong, D. (2015) Synthesis of DNA-Binding Peptoids. Synlett 26, 1581–1585.
- (48) Xia, X., Zhou, Z., DeSantis, C., Rossi, J. J., and Bong, D. (2019) Triplex Hybridization of siRNA with Bifacial Glycopolymer Nucleic Acid Enables Hepatocyte-Targeted Silencing. *ACS Chem. Biol.* 14, 1310–1318.
- (49) Zhou, Z., and Bong, D. (2013) Small-Molecule/Polymer Recognition Triggers Aqueous-Phase Assembly and Encapsulation. *Langmuir* 29, 144–150.
- (50) Zhou, Z., Xia, X., and Bong, D. (2015) Synthetic Polymer Hybridization with DNA and RNA Directs Nanoparticle Loading, Silencing Delivery, and Aptamer Function. *J. Am. Chem. Soc.* 137, 8920–8923.
- (51) Mao, J., DeSantis, C., and Bong, D. (2017) Small Molecule Recognition Triggers Secondary and Tertiary Interactions in DNA Folding and Hammerhead Ribozyme Catalysis. *J. Am. Chem. Soc. 139*, 9815–9818.
- (52) Liang, Y., Mao, J., and Bong, D. (2019) Synthetic bPNAs as allosteric triggers of hammerhead ribozyme catalysis. In *Methods in Enzymology*, Academic Press.
- (53) Tan, X., Constantin, T. P., Sloane, K. L., Waggoner, A. S., Bruchez, M. P., and Armitage, B. A. (2017) Fluoromodules Consisting of a Promiscuous RNA Aptamer and Red or Blue Fluorogenic Cyanine Dyes: Selection, Characterization, and Bioimaging. *J. Am. Chem. Soc.* 139, 9001–9009.
- (54) Yerramilli, V. S., and Kim, K. H. (2018) Labeling RNAs in Live Cells Using Malachite Green Aptamer Scaffolds as Fluorescent Probes. *ACS Synth. Biol.* 7, 758–766.
- (55) Zhang, Y., and Kleiner, R. E. (2019) A Metabolic Engineering Approach to Incorporate Modified Pyrimidine Nucleosides into Cellular RNA. *J. Am. Chem. Soc.* 141, 3347–3351.
- (56) Paredes, E., Evans, M., and Das, S. R. (2011) RNA labeling, conjugation and ligation. *Methods* 54, 251–259.
- (57) Alexander, S. C., Busby, K. N., Cole, C. M., Zhou, C. Y., and Devaraj, N. K. (2015) Site-Specific Covalent Labeling of RNA by Enzymatic Transglycosylation. *J. Am. Chem. Soc.* 137, 12756–12759.
- (58) Dolgosheina, E. V., Jeng, S. C. Y., Panchapakesan, S. S. S., Cojocaru, R., Chen, P. S. K., Wilson, P. D., Hawkins, N., Wiggins, P. A., and Unrau, P. J. (2014) RNA Mango Aptamer-Fluorophore: A Bright, High-Affinity Complex for RNA Labeling and Tracking. *ACS Chem. Biol.* 9, 2412–2420.
- (59) Hecht, S. M. (2000) Bleomycin: new perspectives on the mechanism of action. *J. Nat. Prod.* 63, 158–168.
- (60) Pitié, M., Burrows, C. J., and Meunier, B. (2000) Mechanisms of DNA cleavage by copper complexes of 3-clip-phen and of its conjugate with a distamycin analogue. *Nucleic Acids Res.* 28, 4856–4864.

- (61) Liu, X., Haniff, H. S., Childs-Disney, J. L., Shuster, A., Aikawa, H., Adibekian, A., and Disney, M. D. (2020) Targeted Degradation of the Oncogenic MicroRNA 17–92 Cluster by Structure-Targeting Ligands. J. Am. Chem. Soc. 142, 6970–6982.
- (62) Sigman, D. S., Mazumder, A., and Perrin, D. M. (1993) Chemical nucleases. *Chem. Rev.* 93, 2295–2316.
- (63) Moser, H. E., and Dervan, P. B. (1987) Sequence-specific cleavage of double helical DNA by triple helix formation. *Science* 238, 645–650.
- (64) Dreyer, G. B., and Dervan, P. B. (1985) Sequence-specific cleavage of single-stranded DNA: oligodeoxynucleotide-EDTA X Fe(II). *Proc. Natl. Acad. Sci. U. S. A.* 82, 968–972.
- (65) Breaker, R. R. (1997) DNA aptamers and DNA enzymes. *Curr. Opin. Chem. Biol.* 1, 26–31.
- (66) Carmi, N., Balkhi, S. R., and Breaker, R. R. (1998) Cleaving DNA with DNA. *Proc. Natl. Acad. Sci. U. S. A.* 95, 2233–2237.
- (67) Lee, Y., Klauser, P. C., Brandsen, B. M., Zhou, C., Li, X., and Silverman, S. K. (2017) DNA-Catalyzed DNA Cleavage by a Radical Pathway with Well-Defined Products. *J. Am. Chem. Soc.* 139, 255–261.
- (68) Silverman, S. K. (2010) DNA as a versatile chemical component for catalysis, encoding, and stereocontrol. *Angew. Chem., Int. Ed.* 49, 7180–7201.
- (69) Pratviel, G., Bernadou, J., and Meunier, B. (1998) DNA and RNA Cleavage by Metal Complexes. *Adv. Inorg. Chem.* 45, 251–312.
- (70) Sigman, D. S. (1986) Nuclease activity of 1,10-phenanthroline-copper ion. Acc. Chem. Res. 19, 180–186.
- (71) Zuker, M. (1989) On finding all suboptimal foldings of an RNA molecule. *Science* 244, 48–52.
- (72) Lönnberg, H. (2011) Cleavage of RNA phosphodiester bonds by small molecular entities: a mechanistic insight. *Org. Biomol. Chem.* 9, 1687–1703.
- (73) Nguyen, L., Luu, L. M., Peng, S., Serrano, J. F., Chan, H. Y. E., and Zimmerman, S. C. (2015) Rationally designed small molecules that target both the DNA and RNA causing myotonic dystrophy type 1. *J. Am. Chem. Soc.* 137, 14180–14189.
- (74) Bales, B. C., Kodama, T., Weledji, Y. N., Pitié, M., Meunier, B., and Greenberg, M. M. (2005) Mechanistic studies on DNA damage by minor groove binding copper-phenanthroline conjugates. *Nucleic Acids Res.* 33, 5371–5379.
- (75) Datta, B., and Armitage, B. A. (2001) Hybridization of PNA to structured DNA targets: quadruplex invasion and the overhang effect. *J. Am. Chem. Soc.* 123, 9612–9619.
- (76) Müller, S., Kumari, S., Rodriguez, R., and Balasubramanian, S. (2010) Small-molecule-mediated G-quadruplex isolation from human cells. *Nat. Chem.* 2, 1095–1098.
- (77) Marchetti, C., Zyner, K. G., Ohnmacht, S. A., Robson, M., Haider, S. M., Morton, J. P., Marsico, G., Vo, T., Laughlin-Toth, S., Ahmed, A. A., Di Vita, G., Pazitna, I., Gunaratnam, M., Besser, R. J., Andrade, A. C. G., Diocou, S., Pike, J. A., Tannahill, D., Pedley, R. B., Evans, T. R. J., Wilson, W. D., Balasubramanian, S., and Neidle, S. (2018) Targeting Multiple Effector Pathways in Pancreatic Ductal Adenocarcinoma with a G-Quadruplex-Binding Small Molecule. *J. Med. Chem.* 61, 2500–2517.
- (78) Neidle, S. (2016) Quadruplex Nucleic Acids as Novel Therapeutic Targets. J. Med. Chem. 59, 5987–6011.
- (79) Yu, Z., Fenk, K. D., Huang, D., Sen, S., and Cowan, J. A. (2019) Rapid Telomere Reduction in Cancer Cells Induced by G-Quadruplex-Targeting Copper Complexes. *J. Med. Chem.* 62, 5040–5048.
- (80) Parkinson, G. N., Lee, M. P. H., and Neidle, S. (2002) Crystal structure of parallel quadruplexes from human telomeric DNA. *Nature* 417, 876–880.
- (81) Wang, Y., and Patel, D. J. (1993) Solution structure of the human telomeric repeat d [AG3 (T2AG3) 3] G-tetraplex. Structure 1, 263–282
- (82) Kelley, S., Boroda, S., Musier-Forsyth, K., and Kankia, B. I. (2011) HIV-integrase aptamer folds into a parallel quadruplex: a thermodynamic study. *Biophys. Chem.* 155, 82–88.

- (83) Jing, N., Rando, R. F., Pommier, Y., and Hogan, M. E. (1997) Ion selective folding of loop domains in a potent anti-HIV oligonucleotide. *Biochemistry* 36, 12498–12505.
- (84) Yu, Z., Han, M., and Cowan, J. A. (2015) Toward the Design of a Catalytic Metallodrug: Selective Cleavage of G-Quadruplex Telomeric DNA by an Anticancer Copper–Acridine–ATCUN Complex. *Angew. Chem., Int. Ed.* 54, 1901–1905.
- (85) Cawthon, R. M. (2002) Telomere measurement by quantitative PCR. *Nucleic Acids Res.* 30, No. 47e.
- (86) O'Callaghan, N. J., and Fenech, M. (2011) A quantitative PCR method for measuring absolute telomere length. *Biol. Proced. Online* 13, 3.
- (87) Debacq-Chainiaux, F., Erusalimsky, J. D., Campisi, J., and Toussaint, O. (2009) Protocols to detect senescence-associated beta-galactosidase (SA- β gal) activity, a biomarker of senescent cells in culture and in vivo. *Nat. Protoc. 4*, 1798–1806.
- (88) Phan, A. T. (2010) Human telomeric G-quadruplex: structures of DNA and RNA sequences: Human telomeric G-quadruplex structures. *FEBS J. 277*, 1107–1117.
- (89) Murphy, M. C., Rasnik, I., Cheng, W., Lohman, T. M., and Ha, T. (2004) Probing single-stranded DNA conformational flexibility using fluorescence spectroscopy. *Biophys. J.* 86, 2530–2537.